ISBN: 978-3-95450-184-7 doi:10.18429/JACoW-IPAC2018-THPAK053

SIDE EFFECTS OF LOCAL BUMP IN TPS STORAGE RING

M.S. Chiu†, F.H. Tseng, C.H. Chen, J.Y. Chen and P.J. Chou
National Synchrotron Radiation Research Center, Hsinchu 30076, Taiwan

Abstract

The Taiwan Photon Source (TPS) is a low-emittance 3-GeV light source at National Synchrotron Radiation Research Center. Five in-vacuum undulator beamlines were delivered to users on Sept. 22, 2016. In phase-I insertion device (ID) commissioning, the local bump was used to do ID spectrum optimization. After this procedure, the ID spectrum are consistent between simulation and measurement. Recently, we found the local bump will cause tune shift, orbit distortion, and vertical dispersion by simulation in TPS. These results will be presented in this paper.

INTRODUCTION

TPS [1] storage ring is composed of 24 DBA cells. There are 18 short straight sections (7m) and 6 long straight sections (12m) in storage ring. Three long straight sections are symmetrically configured as double mini-βy lattice. Figure 1 shows the locations of phase-I and phase-II IDs in TPS.

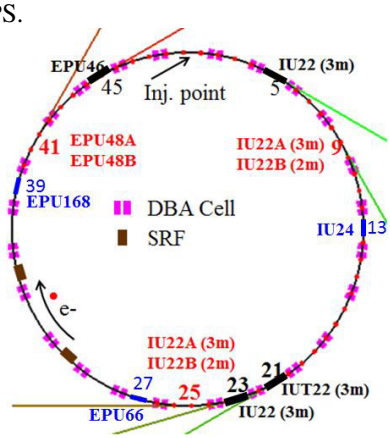

Figure 1: Locations of phase-I and phase-II IDs in TPS storage ring.

In the phase-I ID commissionig [2], a local bump, as illustrated in Fig.4, was used to optimize the ID radiation spectrum. The local bump, combined with the double crystal monochromator (DCM) of the beamline, was used to scan the ID spectrum. For each orbit bump (position or angle), the DCM was used to scan photon energy. After scanning the position and angle bump, the horizontal and vertical orbit were set to the peak of the highest energy curve. According to the formula of radiation wavelength for an undulator, the weaker the magnetic field, the shorter the undulator radiation wavelength. That means the electron orbit traverse through the field center of the ID. Figure 2 and 3 show electron orbit after the optimization of ID spectrum.

† chiu.ms@nsrrc.org.tw

As shown in Figs. 2 and 3, several orbit bumps across quadrupole and sextupole magnets. These orbit bumps will cause tune shifts, orbit distortion and vertical dispersion in the storage ring due to feed-down effects.

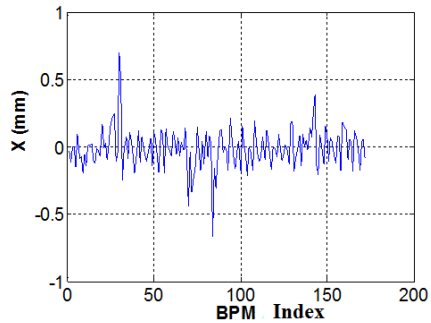

Figure 2: Horizontal orbit after spectrum optimiztion.

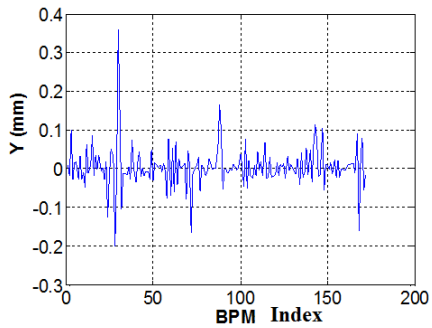

Figure 3: Vertical orbit after spectrum optimization.

LOCAL BUMP

Figure 4 depicts the local bump used to optimize the ID radiation spectrum. The local bump is created by 4 correctors named C1~ C4, adjacent to both sides of ID. These 4 corrector dipoles are trim coils wound on the sextupole magnets S5 and S6, respectively. X and Y are the horizontal and vertical bump height, respectively. X' and Y' are the horizontal and vertical bump angle, respectively.

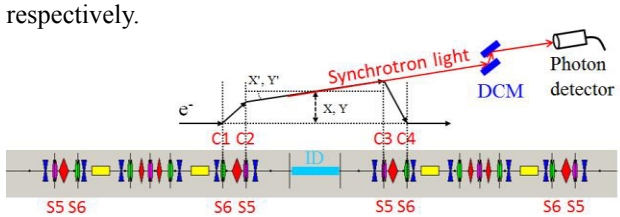

Figure 4: A schematic layout of local bump created to optimize the radiation spectrum of ID.

As shown in Fig. 4, the orbit bump spans across the quadrupole and sextupole magnets. Therefore, the feed-down effects due to orbital offsets in quadrupole and sextupole are created.

ISBN: 978-3-95450-184-7 doi:10.18429/JACoW-IPAC2018-THPAK053

FEED-DOWN EFFECTS

The magnetic fields of a quadrupole are given by

$$B_x = (B\rho)K_1 y,\ B_y = (B\rho)K_1 x \quad (1)$$

, where K_1 is the quadrupole strength, and $B\rho$ is the beam rigidity.

Considering a horizontal orbital offset, we substitute x with $x + \Delta x$ in Eq. (1), we have

$$B_x = (B\rho)K_1 y \quad (2)$$

$$B_y = (B\rho)K_1 \Delta x + (B\rho)K_1 x \quad (3)$$

The first term of B_y in Eq. (3) is a dipole filed, which results in the horizontal orbit distortion.

For a vertical orbital offset, we have

$$B_x = (B\rho)K_1 \Delta y + (B\rho)K_1 y \quad (4)$$

$$B_y = (B\rho)K_1 x \quad (5)$$

The first term of B_x in Eq. (4) is a dipole filed, which results in the vertical orbit distortion.

The magnetic fields of a sextupole are given by

$$B_x = (B\rho)K_2 xy,\ B_y = (1/2)(B\rho)K_2(x^2 - y^2) \quad (6)$$

, where K_2 is the sextupole strength, and $B\rho$ is the beam rigidity.

For a horizontal orbital offset, we have

$$B_x = (B\rho)K_2 y\Delta x + (B\rho)K_2 xy \quad (7)$$

$$B_y = (B\rho)K_2 x\Delta x + (1/2)(B\rho)K_2(x^2 - y^2) + (1/2)(B\rho)K_2\Delta x^2 \quad (8)$$

The first terms of B_x and B_y in Eqs. (7) and (8) are quadrupole fields, which result in tune shifts in both planes. The third term of B_y in Eq. (8) is a dipole field, which results in horizontal orbit distortion.

For a vertical orbital offset, we have

$$B_x = (B\rho)K_2 x\Delta y + (B\rho)K_2 xy \quad (9)$$

$$B_y = (B\rho)K_2 y\Delta y + (1/2)(B\rho)K_2(x^2 - y^2) - (1/2)(B\rho)K_2\Delta y^2 \quad (10)$$

The first terms of B_x and B_y in Eqs. (9) and (10) are skew quadrupole fields, which result in the betatron coupling. The horizontal closed orbit distortion (COD) and dispersion will be coupled to vertical plane. The third term of B_y in Eq. (10) is a dipole field, which results in horizontal orbit distortion.

EFFECTS OF HORIZONTAL BUMPS

Figure 5 shows 20 horizontal orbit bumps ranging from -1 to 1 mm with an increment step of 0.1 mm. Figure 6 shows the corrector strength versus bump height. Figure 7 shows the tune shift versus horizontal bump height. The tune shifts simulated by Tracy [3] are 0.02352 and -0.01098 at a bump height 1 mm in the horizontal and vertical plane, respectively. The value of simulated tune shifts $\Delta\nu_{x,y}$ are consistent with the ones calculated by the formula.

$$\Delta\nu_{x,y} = \frac{\Delta k}{4\Pi}\int_{s_0}^{s_0+l}\beta_{x,y}(s)ds\ ,\ \Delta k = K_2\Delta x \quad (11)$$

, where K_2 is the sextupole strength, and Δx is the orbital offset in sextupole magnet.

Figure 8 shows the horizontal dispersion functions associated with 20 horizontal orbit bumps when the circumference and RF frequency are fixed in the simulations.

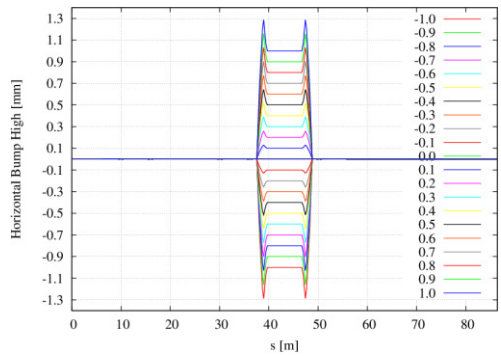

Figure 5: Twenty horizontal orbit bumps ranging from -1 to 1 mm with an increment step of 0.1 mm.

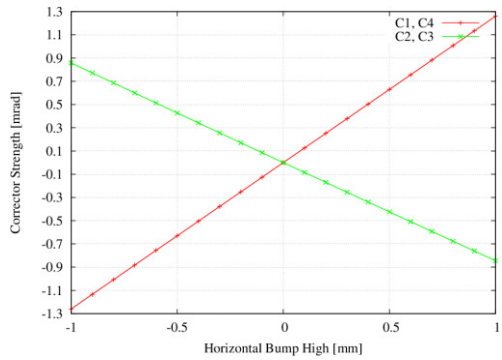

Figure 6: The horizontal corrector strength versus bump height.

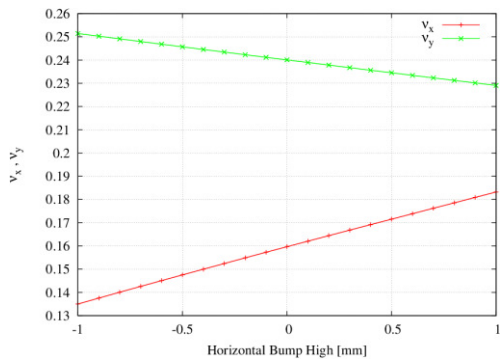

Figure 7: The tune shift versus horizontal bump height.

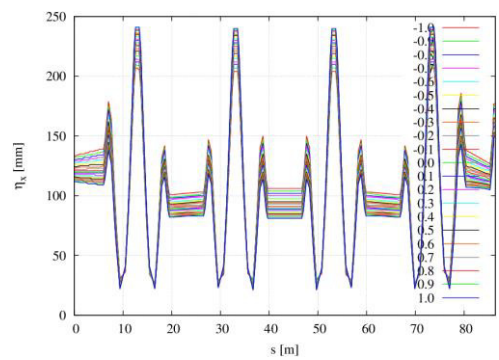

Figure 8: The horizontal dispersion functions associated with 20 horizontal orbit bumps in the simulations.

ISBN: 978-3-95450-184-7 doi:10.18429/JACoW-IPAC2018-THPAK053

EFFECTS OF VERTICAL BUMPS

Figure 9 shows 20 vertical orbit bumps ranging from -1 to 1 mm with an increment step of 0.1 mm. Figure 10 shows the corrector strength versus vertical bump height. Figure 11 shows the tune shift versus vertical bump height. The tune shift is very small. Figure 12 shows the vertical dispersion generated from the skew quadrupole, $K_2\Delta y$, a feed-dwon effect from the vertical orbital offset in sextupole magnets.

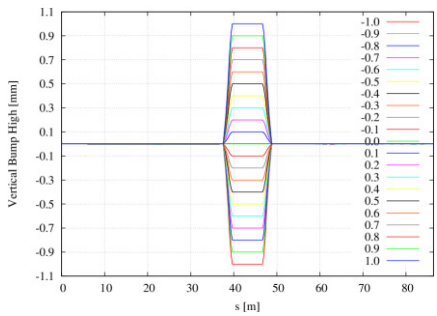

Figure 9: The vertical orbit bumps ranging from -1 to 1 mm with an increment step of 0.1 mm.

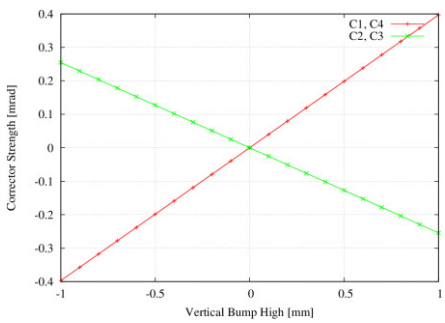

Figure 10: The vertical corrector strength versus vertical bump height.

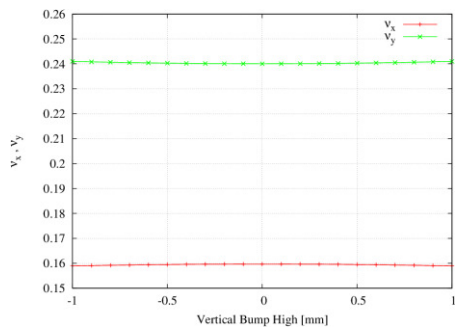

Figure 11: The tune shift versus vertical bump height.

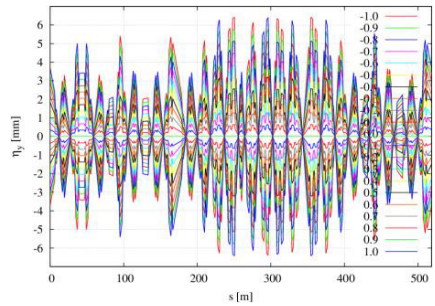

Figure 12: The vertical dispersion generated from the feed-down effect of a vertical orbital offset in sextupole magnets.

For a vertical bump height 1 mm,the horizontal orbit distortion generated from the feed-down effect of a vertical orbital offset in sextupole magnets is shown in Fig. 13.

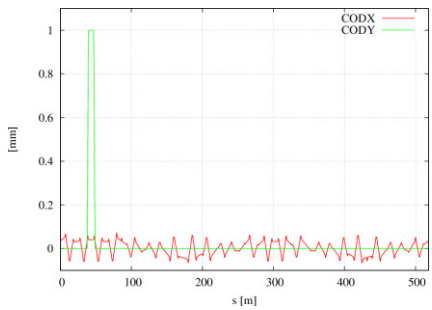

Figure 13: The horizontal orbit distortion generated by the feed-down effect of a vertical orbital offset 1 mm in sextupole magnet.

ACKNOWLEDGEMENT

We would like to show gratitude to those who participate discussions and provide positive suggestions from other group member in NSRRC.

SUMMARY

In phase-I ID commissioning [2], the local orbit bumps were used to optimize the radiation spectrum of ID. After the optimization procedures with local bumps across IDs, the measured radiation spectra of ID are consistent with the simulations. The optimization procedures also create non-neglible orbital offsets in quadrupole and sextupole magnets adjacent to the ID. The feed-down effects of quadrupole and sextupole magnets generte the tune shifts, orbit distortion, and vertical dispersion. These deleterious feed-down effects can be minimized if we choose to align the beamline with respect to the ID instead.

REFERENCES

[1] M.S. Chiu, *et al.*, "Double Mini-Betay Lattice of TPS Storage Ring", in *Proc. IPAC'11*, WEPC035, San Sebastian, Spain, Sept. 2011.

[2] M.S. Chiu, *et al.*, "The Commissioning of Phase-I Insertion Devices In TPS", in *Proc. IPAC'16*, THPMB050, Busan, Korea, May 2016.

[3] TRACY-II, SOLEIL version.